Title

CONDITIONAL VELOCITY STATISTICS IN PREMIXED CH4-AIR AND C2H4-AIR TURBULENT FLAMES

Authors

Cheng, R.K.
Talbot, L.
Robben, F.

Publication Date

1984

Lawrence Berkeley Laboratory
UNIVERSITY OF CALIFORNIA

APPLIED SCIENCE
DIVISION

To be presented at the Twentieth International
Symposium on Combustion, Ann Arbor, MI,
August 12-17, 1984

CONDITIONAL VELOCITY STATISTICS IN PREMIXED CH_4-AIR AND C_2H_4-AIR TURBULENT FLAMES

R.K. Cheng, L. Talbot, and F. Robben

January 1984

APPLIED SCIENCE
DIVISION

Prepared for the U.S. Department of Energy under Contract DE-AC03-76SF00098

DISCLAIMER

Conditional Velocity Statistics in Premixed CH_4-Air and C_2H_4-Air Turbulent Flames

R. K. Cheng, L. Talbot*, and F. Robben

Applied Science Division,
Lawrence Berkeley Laboratory,
University of California,
Berkeley, CA 94720

Mailing Address:

R. K. Cheng
B29C Lawrence Berkeley Laboratory,
University of California,
Berkeley, CA 94720

Subjects:

(1) Turbulent Combustion
(2) Experimental Methods
(3) Flame Shape

* Also Dept. of Mechanical Engineering, University of California, Berkeley, CA 94720

ABSTRACT

Conditioned fluctuation intensities and Reynolds stress have been determined separately for the reactants and for the products in two methane-air and two ethylene-air v-shaped premixed turbulent flames. The conditioned quantities are deduced from velocity data obtained by a two-color LDA system using a conditional analysis method based on the presence of a thin flame sheet dividing the two regions. Within the turbulent flame brush, the conditioned turbulent kinetic energy in the reactants remains at the free stream level. The conditioned turbulent kinetic energy in the products , k_p, are higher than in the reactants indicating flame-generated turbulence. Also, k_p increases with distance from the flame stabilizer, x. Nevertheless, the two conditioned Reynolds stresses are comparable. The unconditioned turbulent kinetic energy and Reynolds stress also increase with x. This increase is proportional to the increase in the difference between the conditioned mean velocities ΔU. The magnitude of ΔU suggests significant stream tube divergence. The results also show qualitative agreement with the model developed by Bray et. al. which relates the difference in the conditioned fluctuation intensities to ΔU.

Introduction

In a recent paper[1], we have described two techniques to measure conditioned turbulence intensity and Reynolds stress in premixed turbulent flames using a two-color laser Doppler anemometry (LDA) system. Conditioned data in the unburned reactants are measured directly by seeding the flow with silicone oil aerosol which evaporates and burns through the flame front. A conditional analysis method is developed to deduce the conditioned data in the burned products from the unconditional data obtained using AL_2O_3 seed particles. The data measured in a premixed v-shaped C_2H_4-air flame show that the apparent increases in turbulence intensity and Reynolds stress within the flame brush are due mainly to intermittency effects caused by the presence of a fluctuating thin flame sheet moving about the measurement point. However, the conditioned data show that the turbulence intensities in the products are generally higher than in the reactant indicating production of turbulence by the flame.

The objective of this paper is to describe and compare the general properties of conditioned turbulence intensity and Reynolds stress measured in two C_2H_4-air and two CH_4-air turbulent flames. Also, the results are used to investigate the modeling assumptions of the turbulence combustion model developed by Bray *et.al.*[2]

Intermittency Model of Flame Turbulence

For typical flame conditions falling into the regime $S_u / u'_\infty > 1.0$ where S_u is the laminar flame speed and u'_∞ is the RMS fluctuation intensity of the incident turbulence, the turbulent flame consists of a thin convoluted flame sheet which fluctuates within the envelope prescribed by the two flame boundaries of the flame brush.[3] This type of turbulent flame, which is usually classified as 'wrinkled laminar flame', is typical of the flames we have studied[4-6]. With respect to an Eulerian reference frame, the flow within the flame brush is intermittent with burned products and unburned reactants separated by the flame sheet acting as an interface. Under fast chemistry and thin flame assumptions, the probability of the intermediate state is therefore comparatively small. The velocity statistics can then be described by an intermittency model similar to the one developed by Bray et. al.[2] The Eulerian averaged (unconditioned) mean velocities, $\bar{U}$ and $\bar{V}$, are expressed in terms of of an intermittency factor Ω,and the two corresponding conditioned mean velocities in the reactants and in the products, subscripted r, and p respectively :

$$\bar{U} = (1 - \Omega) \bar{U}_r + (\Omega) \bar{U}_p \tag{1}$$

and

$$\bar{V} = (1 - \Omega) \bar{V}_r + (\Omega) \bar{V}_p \tag{2}$$

Ω represents the probability of the products which varies from 0.0 in the reactants to 1.0 in the products. Similarly, the mean square of the velocity fluctuations are

$$(u')^2 = (1 - \Omega) (u'_r)^2 + \Omega (u'_p)^2 + \Omega (1 - \Omega) (\bar{U}_p - \bar{U}_r)^2 \tag{3}$$

and

$$(v')^2 = (1 - \Omega) (v'_r)^2 + \Omega (v'_p)^2 + \Omega (1 - \Omega) (\bar{V}_p - \bar{V}_r)^2 \tag{4}$$

The covariance (Reynolds stress) is then

$$\overline{uv} = (1 - \Omega) (\overline{uv})_r + \Omega (\overline{uv})_p + \Omega (1 - \Omega)(\bar{U}_p - \bar{U}_r)(\bar{V}_p - \bar{V}_r) \tag{5}$$

In these equations, Ω appears as a weighting factor or conditioning function. In the model of Bray et.al.[2] for the Favre averaged turbulence quantities, the conditioning function is the Favre averaged conserved scalar c. Note that the last term in Eqs. (3)-(5) refers only to the mean conditioned velocity and not to the turbulence components.

This contribution to fluctuation intensity and covariance arises in the Eulerian description of the flame turbulence, due to the effect of intermittency. The Lagrangian description of the flame turbulence only includes the first two conditioned terms.

Experimental System

The experimental set-up is shown schematically in Fig. 1. The turbulent flame is stabilized by a 1.0 *mm* diameter rod placed at the exit of a flow nozzle which provides a circular co-axial jet with an inner core of fuel/air mixture 5.0 *cm* in diameter surrounded by an annular air jet of 10.0 *cm* outer diameter. Incident turbulence is generated either by a bi-plane grid of 5.0 *mm* square mesh with 1.0 *mm* elements or a perforated plate with 3.2 *mm* circular holes spaced 4.8 *mm* apart. The turbulence generator is placed 50 *mm* upstream of the stabilizer.

A Spectra-Physics 2.0 watt argon-ion laser is the light source for the four-beam two color LDA system. Differential frequency shifting by Bragg cells is used for measuring the transverse velocity, V. The collection optics consists of two photomultiplier assemblies placed in the forward scattered direction at approximately $\pm 10^{o}$ from the optical axis. The laser, the LDA optics and the collecting optics are mounted on a computer-controlled three axis traverse table to facilitate rapid scanning of the flame.

To directly obtain conditional sampling in the unburned reactants, silicone oil aerosol provides the LDA seed particles. The aerosol is generated by an air jet atomizer using Dow Corning silicone oil made. Previous flow visualization results[7] have shown that these oil droplets are evaporated and burned through the thin flame. Consequently, the LDA measurements made with silicone oil droplets refer only to the reactants ahead of the flame sheet. For sampling unconditionally through the flame, aluminum oxide particles of 0.3 μm are introduced into the flow by a cyclone canister seeder.

The Doppler bursts are analyzed by two TSI 1980A frequency counters interfaced with a data acquisition system based on a PDP 11/10 computer. Digitizing and recording of the counter outputs are triggered by a co-validation circuit. The criterion for

coincidence is that the two counter signals arrive within 3.0 μsec of each other. At every measurement position, a series of instantaneous velocity vectors $\vec{U}(n)=U(n)+V(n)$, $n=1...4096$ are recorded and stored on magnetic tape for reduction on the LBL CDC 7600 computer. Velocity profiles consisting of 30 points are made at six locations from x = 10 to $60mm$ above the stabilizer at $10.0mm$ interval. More details of the LDA system and data acquisition system are included in Ref. 1, where the effects of various biasings on these data are also discussed.

Data Analysis

The conditional analysis method to obtain the two conditioned quantities from the unconditioned velocity data is described more conveniently with reference to the velocity Joint Probability Density Functions (JPDF) shown in Fig. 2. Compared here are the contours of the JPDF's within the flame brush obtained with the use of silicone oil aerosol (conditioned reactant), $p_r(U,V)$, and with Al_2O_3 (unconditioned), $p(U,V)$. It is obvious that $p(U,V)$ is double-peaked and $p_r(U,V)$ is single-peaked. Furthermore, the single $p_r(U,V)$ peak corresponds to one of the peaks of $p(U,V)$. Therefore, the second (lower) peak on $p(U,V)$ must be associated with the burned products. A conditional function, $g(U,V)$ can then be introduced to compute the conditioned velocity statistics from $p(U,V)$ such that

$$\overline{U}_r = \frac{\int\int U\, g(U,V)\, p(U,V)\, dU\, dV}{\int\int g(U,V)\, p(U,V)\, dU\, dV} \tag{6a}$$

and

$$\overline{U}_p = \frac{\int\int U\,(1-g(U,V))\, p(U,V)\, dU\, dV}{\int\int g(U,V)\, p(U,V)\, dU\, dV} \tag{6b}$$

where $g(U,V)$ satisfies

$$g(U,V) = \begin{cases} 1 & \text{if } U<U_{\text{lim}}, \text{ and } V<V_{\text{lim}} \\ 0 & otherwise \end{cases}$$

The criteria for U_{lim} and V_{lim} can be determined on the $U-V$ plane by the extent of the $p_r(U,V)$ contours. For example, U_{lim} and V_{lim} shown in Fig. 2 are $6.5m/s$ and $0.05m/s$ respectively. Note that Eq. (6a) should be equivalent to

$$\overline{U}_r = \int\int U\, p_r(U,V)\, dU\, dV$$

To compute the conditional mean velocities form the data series $\vec{U}(n)$, the following equations are used:

$$\overline{U}_r = \frac{1}{N_r} \sum_{n=1}^{4096} g(U,V)\ U(n) \tag{7a}$$

and

$$\overline{U}_p = \frac{1}{N_p} \sum_{n=1}^{4096} (1-g(U,V))\ U(n) \tag{7b}$$

where N_r is the number of data satisfying $g(U,V)=1$, and N_p is the number of data satisfying $g(U,V)=0$. Similar expressions are used to compute the conditioned fluctuation intensity and the covariance. The accuracy of the analysis is inferred by comparing the conditioned statistics obtained for the reactants with similar data measured using silicone aerosol. As shown in the previous paper[1], the results of the conditional analysis compare very well with measured data even at positions close to the product where N_r is small and the uncertainties of the analysis are expected to be high. Therefore, the data obtained from direct conditional sampling using silicone oil are not presented here. Only the results obtained from conditional analysis are discussed.

Results

The mixture compositions and experimental conditions of the four flames are listed in Table I. The methane-air and the ethylene-air mixtures are arranged to have the same laminar burning velocity, S_u,[8] so that the differences in the reaction of the methane and ethylene flames to identical incident turbulence can be shown. The unburned/burned density ratios of the ethylene-air and methane-air mixtures are about 7.8 and 8.3 respectively.

The overall geometry of the four flames is compared in Fig. 3 and 4. In Fig. 3, the orientation of the flame brush is shown by the locus of the positions of maximum turbulence kinetic energy, k_{max} where $k \equiv \frac{1}{2}(u'^2+v'^2)$. These loci show that the orientations of No. 1,2 and 4 are quite similar while No. 3 is more oblique to the incident flow. The flame brush thickness, δ_t, is shown in Fig. 4. At $x = 20mm$, δ_t for No. 1 and 3 are about $2.0mm$ while δ_t for No. 2 and 4 are larger at about $4.0mm$. The larger δ_t of No. 2 and 4

is consistent with schlieren observation showing that the flame convolutions are developed closer to the flame stabilizer in these flames with higher incident turbulence. The growth rate of No. 3 is quite linear reaching to $\delta_t = 6.0mm$ at $x=60mm$. The most rapid growth rate is shown by No. 1. At $x=60mm$, δ_t for No. 1,2 and 4 are about $11mm$. As shown by the flame orientations and flame brush thicknesses, the features of the methane and ethylene flame subjected to incident turbulence are indeed different.

Note that the typical laminar flame thickness, δ_l, for these flames is about $1.0mm$.[9] If $\delta_t \approx \delta_l$, the probability of the intermediate states becomes much higher, therefore the assumptions of the intermittency model are not valid. This occurs at positions close to the flame stabilizer. As a result, conditional analysis of the data is possible only at $x \geq 30mm$ for No. 1 and 3, and at $x \geq 20.0mm$ for No. 2 and 4.

Representative JPDF's from each flame are shown in Fig. 5. The double peak feature is common to all the JPDF's though the shapes of the contours are different. Note that the contours of the two peaks are separate for No. 1,3 and 4, and only slightly interconnected for No. 2, indicating the low probability of intermediate states. The locations of the product peaks at regions of higher U indicate axial acceleration of the flow in the product. Since all the reactant peaks are mostly within the positive V region while the product peaks are in the negative V region, the overall effect of the flame-flow interaction is to deflect the flow from outward to inward towards the flame center. This is consistent with the model of a thin wrinkled flame through which the tangential velocity component is conserved.[6]

The difference between the conditioned mean velocity vectors, $\Delta U = ((\bar{U}_p - \bar{U}_r)^2 + (\bar{V}_p - \bar{V}_r)^2)^{1/2}$ at k_{max} (i.e. the positions of Fig. 2) are compared in Fig. 6. This parameter represents the overall flow acceleration across the flame and is also proportional to the intermittency contribution to the fluctuation intensities since the sum of Eq.(2) and (3) is $2k = 2(1-\Omega)k_r + 2\Omega K_p + \Omega(1-\Omega)\Delta U^2$. As shown here, ΔU increases with x. However, ΔU is found to be relatively constant across the flame brush in the transverse direction y. Although the reactant/product density ratio of the mixtures

are about the same, the differences in ΔU for the flames are quite large. The lowest ΔU is found for No. 3. It increases by only about $0.2m/s$ along the flame brush. In contrast, for No. 1 with identical incident turbulence but with ethylene, ΔU is substantially higher and increases rapidly to a plateau at x=50mm. The difference in ΔU for No. 2 and 4 are less drastic. However, a maximum is shown for No. 2 at x=40.0mm. Note that the results for No. 1 and 4 are quite similar and do not show any local maxima such that at x>50mm they exceed ΔU for No. 2.

In Fig. 7, k_{max} along the flames are shown. At these positions where $\Omega \approx 0.5$, the contributions from ΔU are most significant. Therefore, it is not surprising to find that k_{max} also increases with x. Up to $x \leq 30mm$ the results show that under similar incident turbulence, k_{max} within ethylene flames are higher than in the methane flames. At $x \geq 50mm$, this difference becomes less consistent since k_{max} for No. 1,2 and 4 are more comparable. The fluctuations within the flame brushes are slightly anisotropic with v' generally higher than u'.

The corresponding conditioned turbulent kinetic energies, k_r, and k_p are shown in Fig. 8. The k_r's are found to be approximately equal to the incident turbulence. For No. 2,3 and 4, k_r decays slightly with increasing x while for No. 1 the results show a very small increase.

The turbulent kinetic energies in the products, k_p, are higher than k_r, and increase with increasing x. We regard the higher turbulence levels in the products as an indication of the true 'flame generated turbulence', since these quantities do not include the effects of intermittency. In general, higher incident turbulence level produces higher k_p shown here by the difference between the results of No. 1 and 2, and No. 3 and 4. However, with similar incident turbulence, k_p in the ethylene flames are consistently higher than in the methane flames except at x>50mm where k_p for No. 4 exceeds that of No. 2. More discussion of this interesting feature is included in the next section. These results again show the differences between the methane and ethylene turbulent flames. The k_p's are all lower than k_{max}. However, at some transverse positions close to the flame boundaries k_p sometimes exceeds the

corresponding k.

In the paper by Bray et. al.[2], the difference in the conditioned mean velocity is used to model the difference in the conditioned turbulence intensities. For their one-dimensional turbulent flame, the model is $(u'_p)^2-(u'_r)^2=\kappa_3(\bar{U}_p-\bar{U}_r)^2$ where κ_3 is an empirical constant. Since our turbulent flames are two-dimensional, the analogous formula would be

$$k_p - k_r = \kappa_3 \tfrac{1}{2}(\Delta U)^2$$

It is interesting to note that since k_r is relative constant with x, qualitative support of this model is shown by the similarity between the shapes of the ΔU and k_P curves. The values of κ_3 obtained for k_{max} are listed in Table II. The results show that κ_3 increases with x, and the values for No. 1,2 and 4 are about twice that for No. 3. However, the value of 0.1 used in the work of Bray et. al.[2] falls within the range of the results. Although this comparison does not provide a consistent value of κ_3, it does show, at least qualitatively, that the model proposed by Bray et. al. is indeed a useful approximation of the conditioned turbulence intensities.

The conditioned and unconditioned covariances are shown in Fig. 9 and 10 respectively. Fig. 9 shows that all $(\overline{uv})_r$ are close to zero. The values of $(\overline{uv})_p$ for No. 1 and 3 are close to zero, and are less than $0.05(m/s)^2$ for No. 2 and 4. The $(\overline{uv})_p$ results demonstrate again that the 'flame generated turbulence' is not associated with additional shear stress. In contrast, the values of $\overline{uv}$ shown in Fig. 10 are all negative and substantially higher than the conditioned results. As discussed in our previous papers,[1,6] the sign of the covariance is opposite to that predicted by mean gradient transport model. It is obvious from Eq. (5) that the major contribution to the covariance is from the intermittency term. The sign of the contribution is consistent with the difference in the mean conditioned velocities. Since $(\bar{V}_P-\bar{V}_r)$ is negative and $(\bar{U}_p-\bar{U}_r)$ is positive, their product is negative. In fact, the magnitudes of $\overline{uv}$ shown in Fig. 9 are essentially equal to $0.25(\bar{V}_p-\bar{V}_r)(\bar{U}_p-\bar{U}_r)$. These results again demonstrate that the mean gradient transport model is not highly appropriate for premixed turbulence flames.

Discussion

The differences in the flame geometry and fluctuation intensities in the methane and ethylene flames indicate that incident flow properties such as U_∞, u'_∞, the length scales and S_u are not sufficient to prescribe the characteristics of a turbulent flame. The extent of the heat release which is proportional to the product/reactant density ratio should also be of significance. However, the overall features of the conditioned fluctuation intensities and covariances are similar. The fluctuation intensities in the reactants remain comparable to the incident turbulence level The conditioned fluctuations in the products are higher but are not associated with an increase in shear stress. In three cases, the turbulence kinetic energies in the products k_p continuously increase with x.

The results for No. 2 show a slight decrease at $x>50mm$ following the initial increase. Visual observation indicates that this flame has the shortest flame height due to the high incident turbulence and enlarged flame brush thickness. Also, the flame sheet farther away from the stabilizer becomes so convoluted that occasionally large swells of flame pockets are shown.[6] The decrease at $x>50mm$ may be typical of the flame properties approaching the tip of the flame brush. It is of interest to note that the results of No. 1 seems to exhibit a similar trend at $x=60mm$. Although the results of No. 3 and 4 do not show any level-off or decrease, it seem reasonable to suspect that the fluctuations will eventually decrease.

The initial increase in k_p with x seems to support the argument that the turbulence production may be kinematic in nature, as suggested in an early paper by Karlovitz et. al.[10] This argument correlates the increase in k_p with the increase in flame wrinkle. The interaction of the incident flow with the curved flame can result in more random flow deflections which increases the fluctuation intensities in the product. Our results show that the increase in k_p is consistent with the growth of the flame brush thickness as the flame sheet becomes more convoluted. Comparison of the experimental results with theoretical calculations using the vortex dynamics model[11] will help to determine whether or not turbulence production by this mechanism is significant.

Another parameter which could be of importance to the understanding of turbulence flame propagation is ΔU. Its significance has been recognized by Bray et. al. in their model.[2] Our data show that ΔU generally increase with x and incident turbulence. The variation of ΔU seems to suggest combustion induced stream-tube divergence. Since ΔU represents the overall change in mean flow velocity across the flame, the conservation of mass can be approximated by $(\Delta U / S_t)+1=\rho_r A_r / \rho_p A_p$, where S_t is the turbulent burning velocity. For these turbulent flames, the turbulent burning velocity is about twice the laminar burning speed ($S_t \approx 2S_u = 0.8 m/s$) such that the ratio $\Delta U / S_t$ is less than 2.5. Using reactant/product density ratio of 8.0 indicates that $A_p > A_r$. As ΔU becomes smaller close to the stabilizer or when the flame is oblique as in No. 3, the divergence would be more significant. The most interesting implication of this interpretation is that the decrease in flow divergence is associated with an increase in turbulence production which, may also be related to the development of the flame wrinkles. Further investigation of this feature of the oblique turbulent flame may require comparison with data obtained in oblique laminar flames.

Finally, the variation of turbulence properties along the flame shows that the flow-fields of these simple planar unconfined v-shaped flames are highly two dimensional. To compare the experimental results with a one-dimensional theoretical model requires a co-ordinate transformation of the data. The selection of the flame co-ordinate for transformation is not trivial and would need careful consideration. For example, the overall orientation of the flame brush associated with the loci of Fig. 2 is in general smaller than the direction of maximum flow acceleration as indicated by ΔU. Therefore, these two logical choices for co-ordinate transformation to obtain one dimensional turbulence properties would produce quite different results, especially with regard to the shear stress across the flame. This aspect of turbulent flame study is being pursued and the results will be forthcoming.

Conclusions

A two-color LDA system is used to study premixed turbulent flame propagation in two methane-air and two ethylene-air v-shaped flames. The results are analyzed to

obtain conditioned velocity fluctuation intensities and covariances. These conditioned quantities in the reactants and in the products are useful for comparison with either the Lagrangian or Eulerian models of turbulent combustion. The results of the analysis are found to compare well with direct measurement of the conditional properties in the reactants.

Under similar incident turbulence, and with the methane and ethylene mixtures having the same laminar burning speed, the overall geometry and the fluctuation intensity of the two flames are different. However, the behavior of the turbulence properties across the flame are similar. The conditioned fluctuation intensities in the reactants remain comparable to the incident turbulence level. The fluctuation intensities in the products generally increase with distance from the stabilizer, and are higher than those in the reactants, indicating production of turbulence by the flame. However, this increase in turbulence is not associated with an increase in shear stress because the covariance (Reynolds stress) in the products is comparable to that in the reactants.

The peak unconditioned fluctuation intensity and covariance also increase with x. This increase is proportional to the increase in the difference between the conditioned mean velocities, ΔU. The magnitude and change in ΔU implies that combustion induces stream-tube divergence across the flame, and that the divergence is more significant closer to the stabilizer. This observation suggest possible relationship between the flow divergence and the production of turbulence.

The results are compared with the model developed by Bray et. al. relating the difference in the conditioned fluctuation intensities to ΔU. Although our data do not provide a consistent value of the empirical constant, qualitative agreement is found.

Acknowledgement

The authors would like to acknowledge the assistance of Mr. Edward Stracke for preparing some of the illustrations. This work was supported by the Director, Office of Energy Research, Office of Basic Energy Sciences, Chemical Sciences Division of the U.

S. Department of Energy under Contract No. DE-AC-03-76SF00098.

References

1. Cheng, R. K., "Conditional Sampling of Turbulence Intensities and Reynolds Stress in Premixed Turbulent Flame," Lawrence Berkeley Laboratory Report LBL-16938 (1983). Also submitted for publication in *Combustion Science and Technology* , (1983).

2. Bray, K. N. C., Libby P. A., Masuya, G. and Moss, J. B. *Combustion Science and Technology, 25* , 127 (1981).

3. Andrews, G. E., Bradley, D., and Lawkabamba, S. B., *Combustion and Flame, 24*, 285 (1975).

4. Bill, R. G., Jr., Namer, I., Talbot, L., Cheng, R. K., and Robben, F.: *Combustion and Flame, 43* , 3, 229 (1982).

5. Namazian, M., Talbot, L., Robben, F., and Cheng, R. K.: *Nineteenth Symposium (Int'l) on Combustion* ,p. 487, The Combustion Institute (1983).

6. Cheng, R. K., and Ng, T. T.: *Combustion and Flame, 52* ,p. 185 (1983).

7. Hertzberg, J. R., Namazian, M. and Talbot, L. to appear in *Combustion Science and Technology* (1984).

8. Raezer, S. D., and Olsen, H. L. *Combustion and Flame, 6*, 456 (1961).

9. Namazian, M., Talbot, L. Robben, F, "Deinsity Fluctuations in a Rod-Stablized Premixed Turbulent Flame," Paper submitted to the *Twentieth International Symposium on Combustion* , Aug. 12-17 (1984).

10. Karlovitz, B., Dennison, D. W., and Wells, F. E. *J. Chem. Phys., 12* , 5, 541 (1951).

11. Ashurst, Wm. T. and Barr, P. K. To be published in *Combustion Science and Technology* (1983).

TABLE I Experimental Conditions

No.	fuel	Equiv. ratio	U_∞ (m/s)	turb. source	$(u'/U)_\infty$ (%)	$(v'/U)_\infty$ (%)	Fig. symbol
1	C_2H_4	0.7	5.5	grid	5.0	5.0	●
2	C_2H_4	0.7	5.5	plate	7.0	5.5	○
3	CH_4	0.83	5.5	grid	5.0	5.0	▲
4	CH_4	0.83	5.5	plate	7.0	5.5	Δ

Table II Values of κ_3 at k_{max}.

	$x(mm)$ 20.0	30.0	40.0	50.0	60.0
No. 1		0.18	0.23	0.26	0.28
2	0.12	0.26	0.41	0.36	0.35
3		0.08	0.09	0.16	0.12
4	0.03	0.12	0.21	0.27	0.33

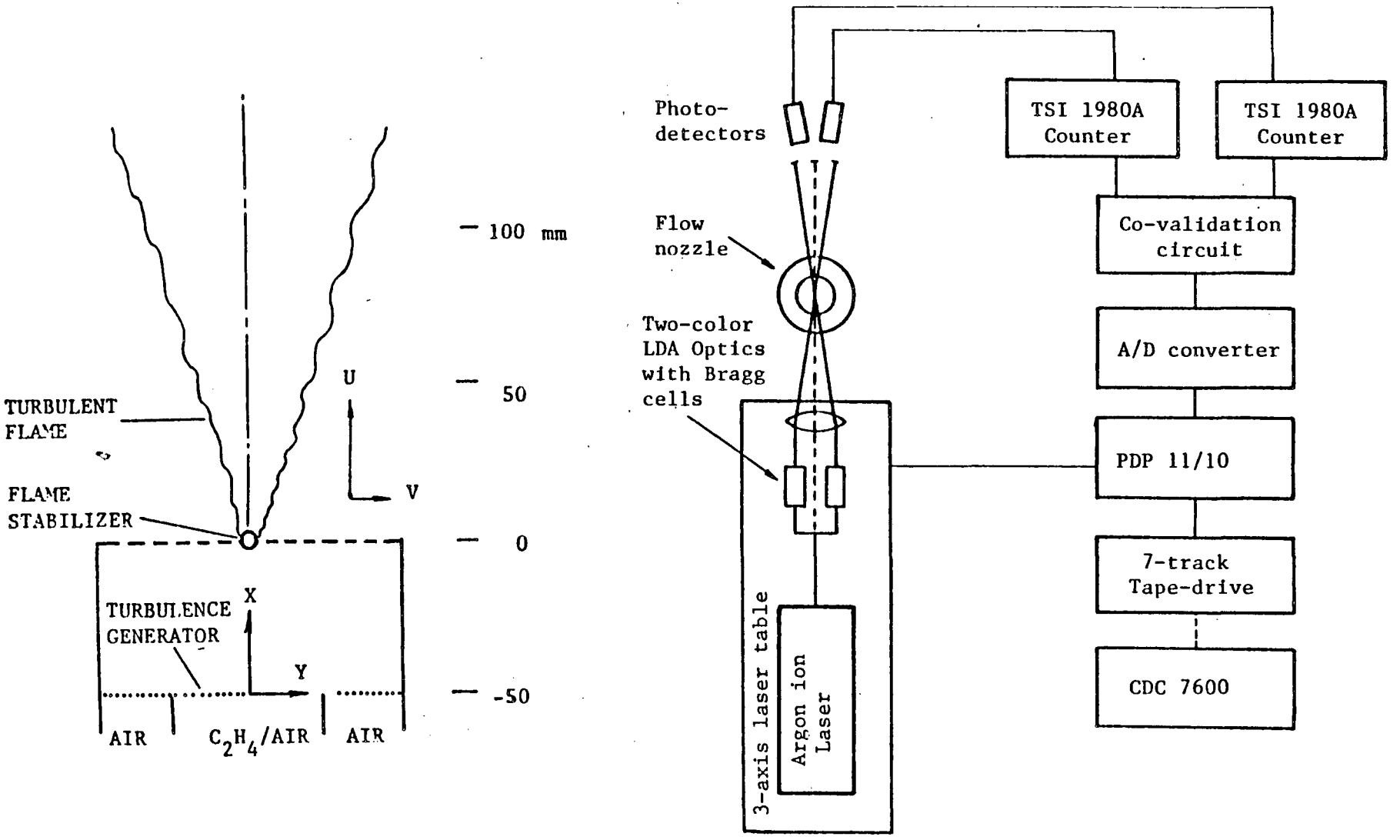

Fig. 1 Schematics of the experimental and data acquisition system

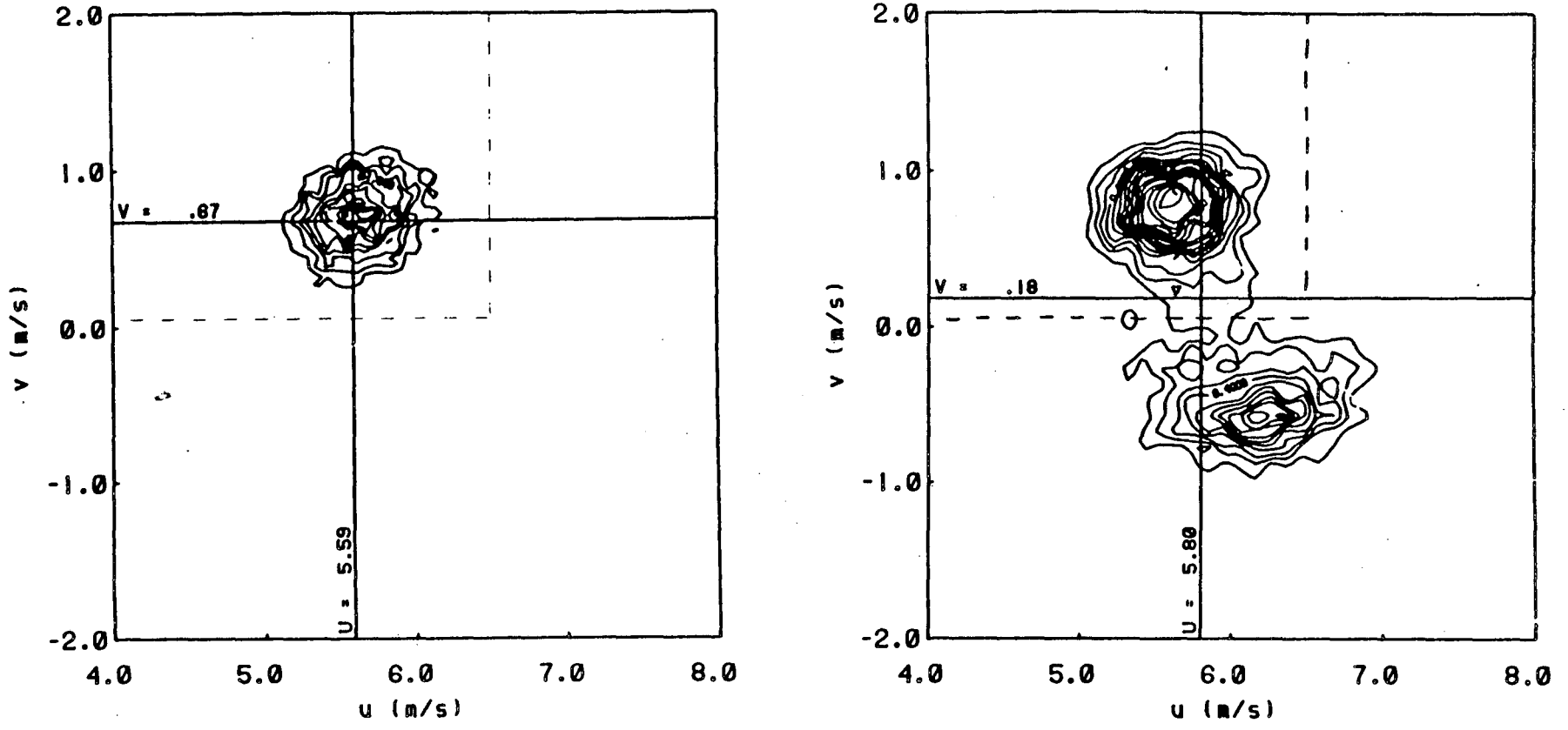

Fig. 2 Contour plots of (a) the conditioned JPDF in the reactants and (b) the unconditioned JPDF obtained for flame No. 1 at x=30mm and y=8.0mm. Contour lines are shown for every 10% of the maximum value of the JPDF. The broken lines show V_{lim} and U_{lim} associated with the conditional function $g(U,V)$.

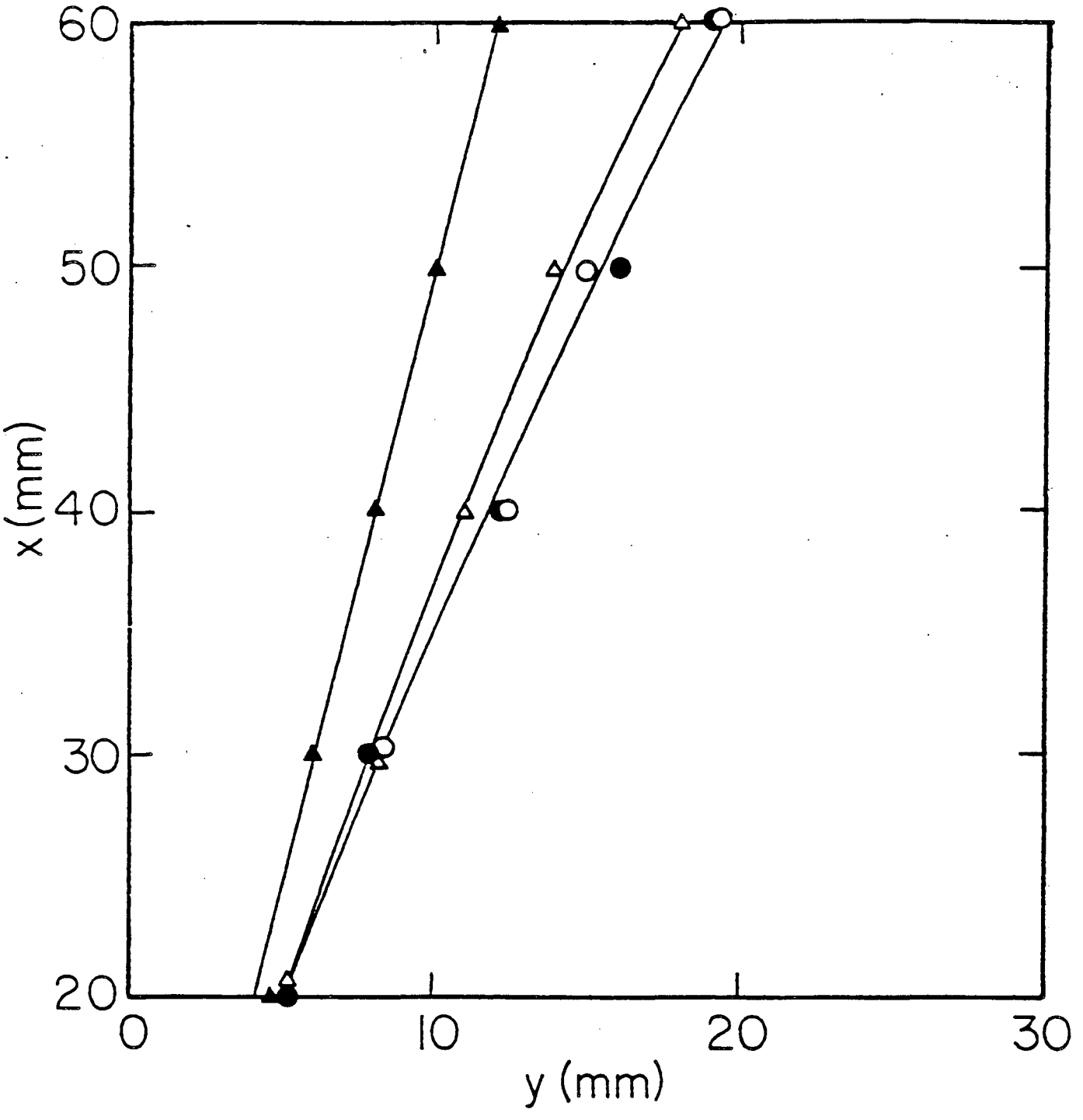

Fig. 3 Loci of the positions of maximum turbulent kinetic energy, k_{max} within the flame brushes. No. 1, ; No. 2, ○, No. 3, ▲; No. 4, Δ.

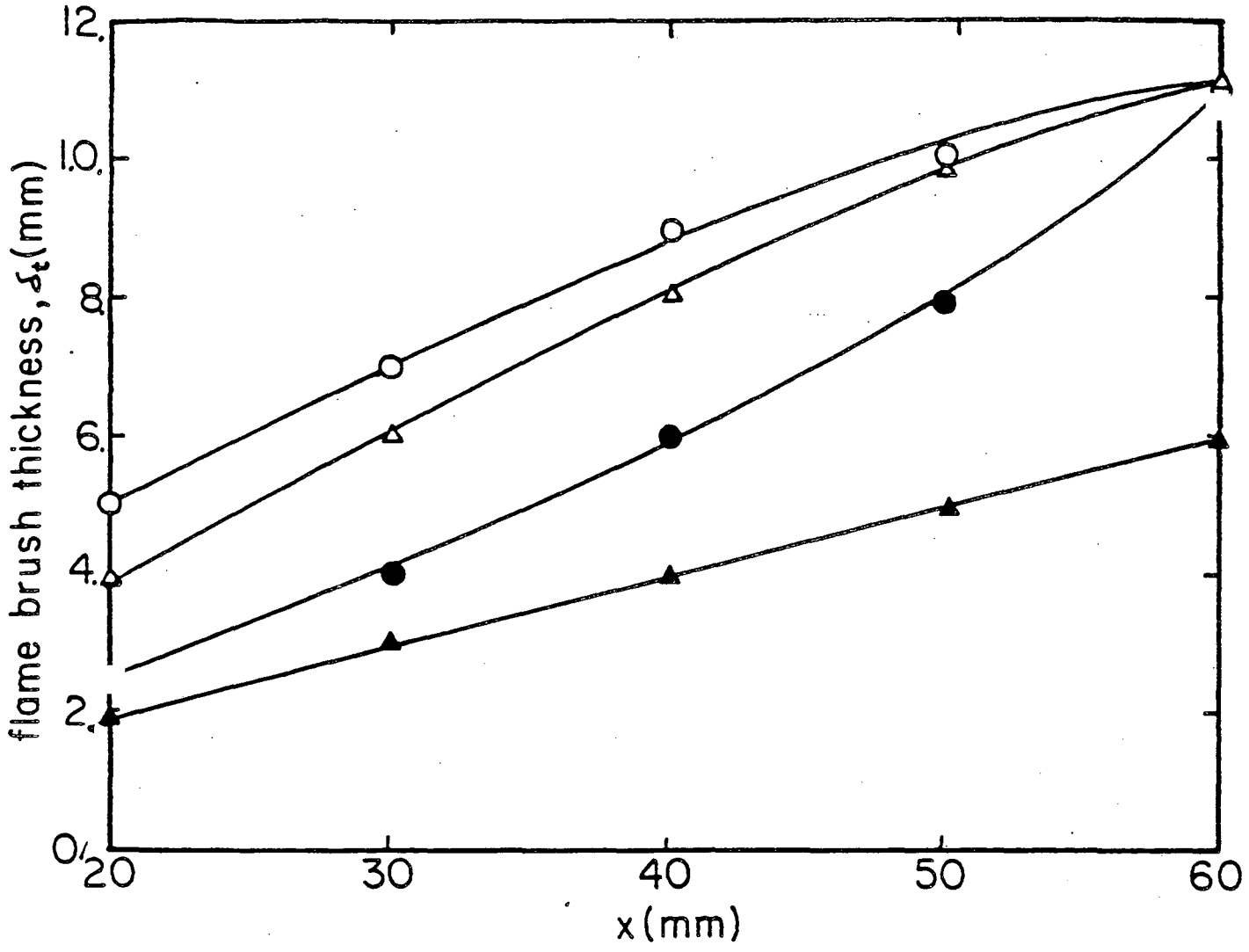

Fig. 4 Flame brush thickness δ_t as function of x. No. 1, ●; No. 2, ○, No. 3, ▲; No. 4, Δ.

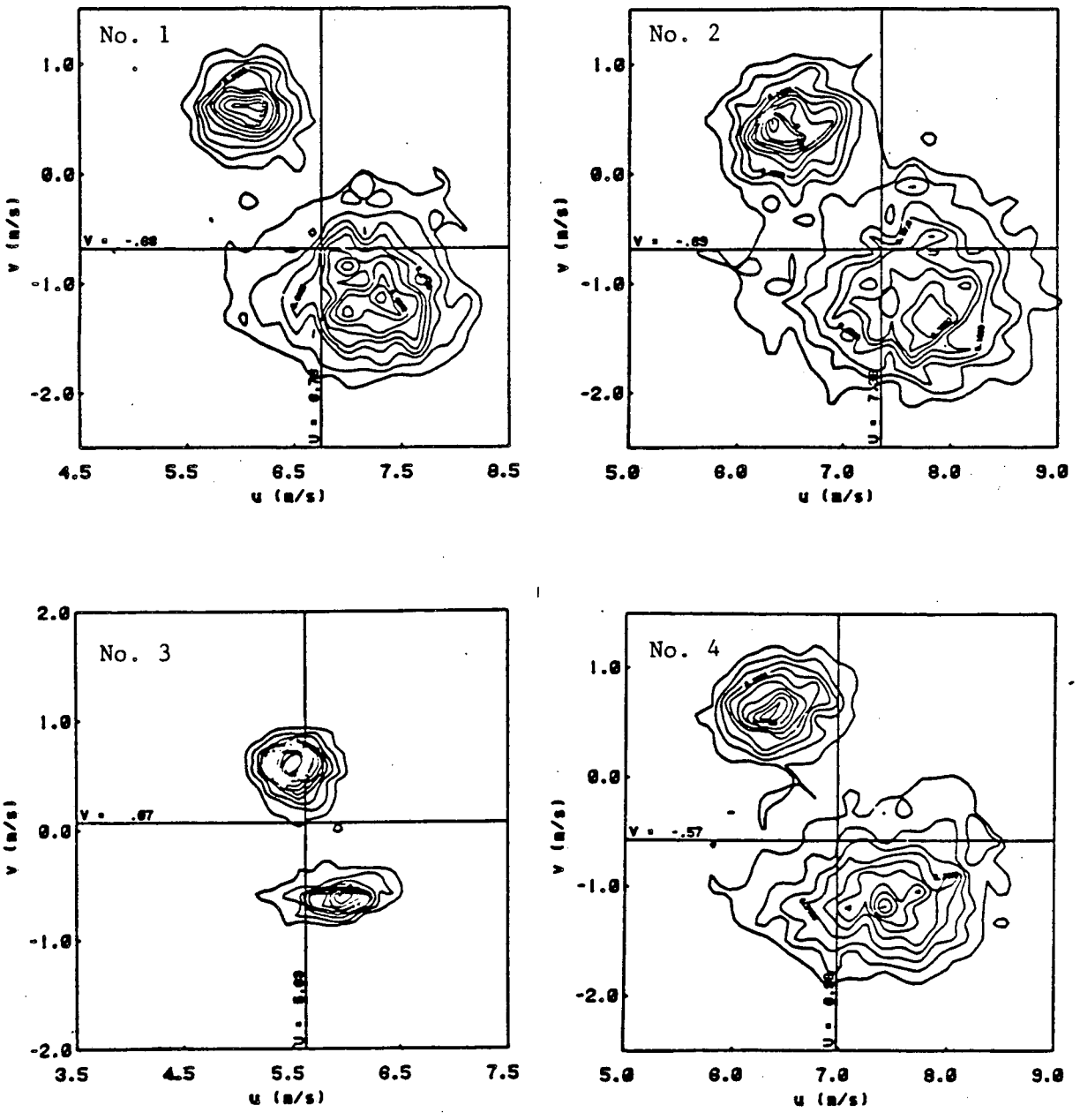

Fig. 5 Comparison of the JPDF obtained for each flame at x=50mm and position of k_{max}. Contour lines are shown for every 10% of the maximum value of the JPDF.

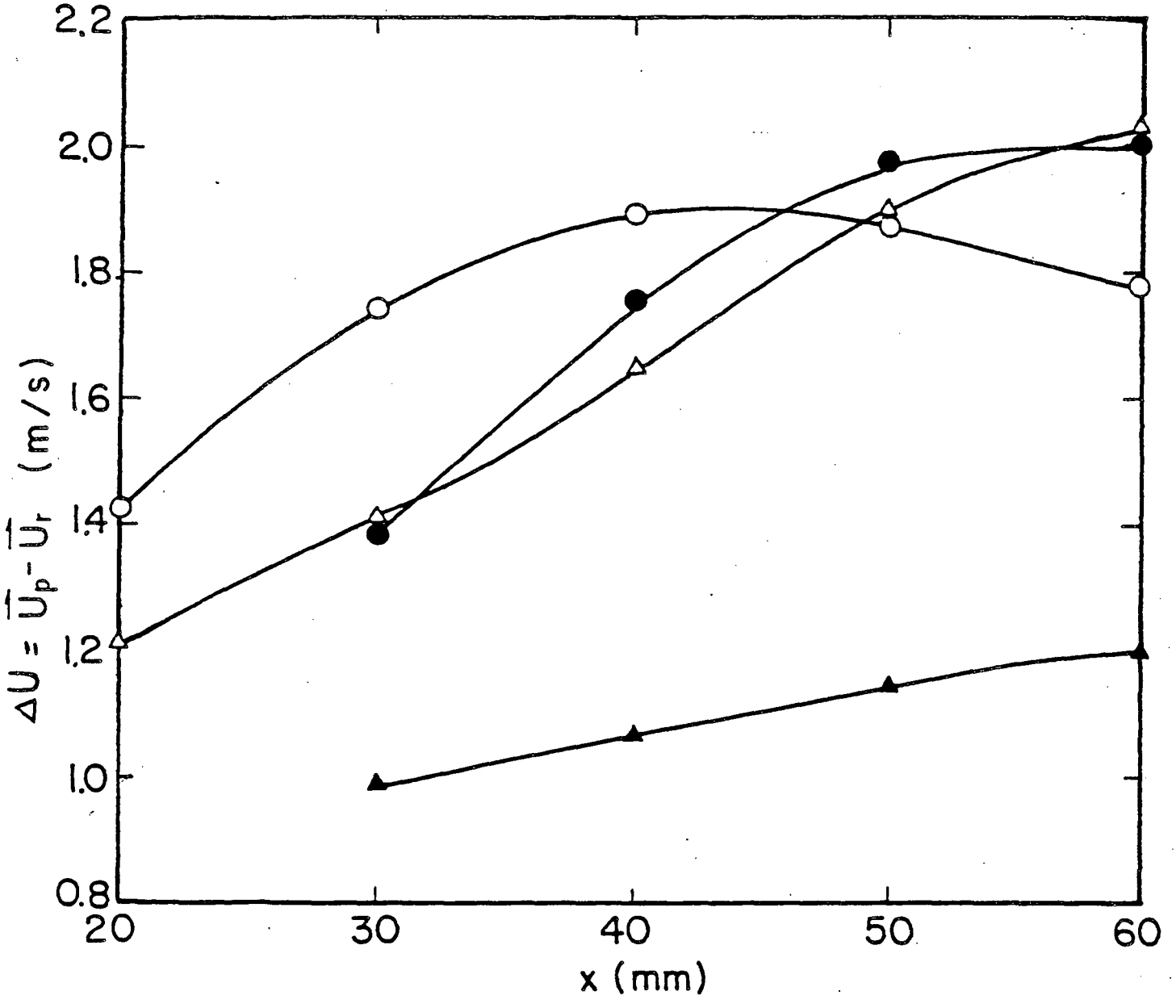

Fig. 6 The difference in conditioned mean velocity in the reactnats and in the products, ΔU, along the k_{max} loci. No. 1, ●; No. 2, ○, No. 3, ▲; No. 4, Δ.

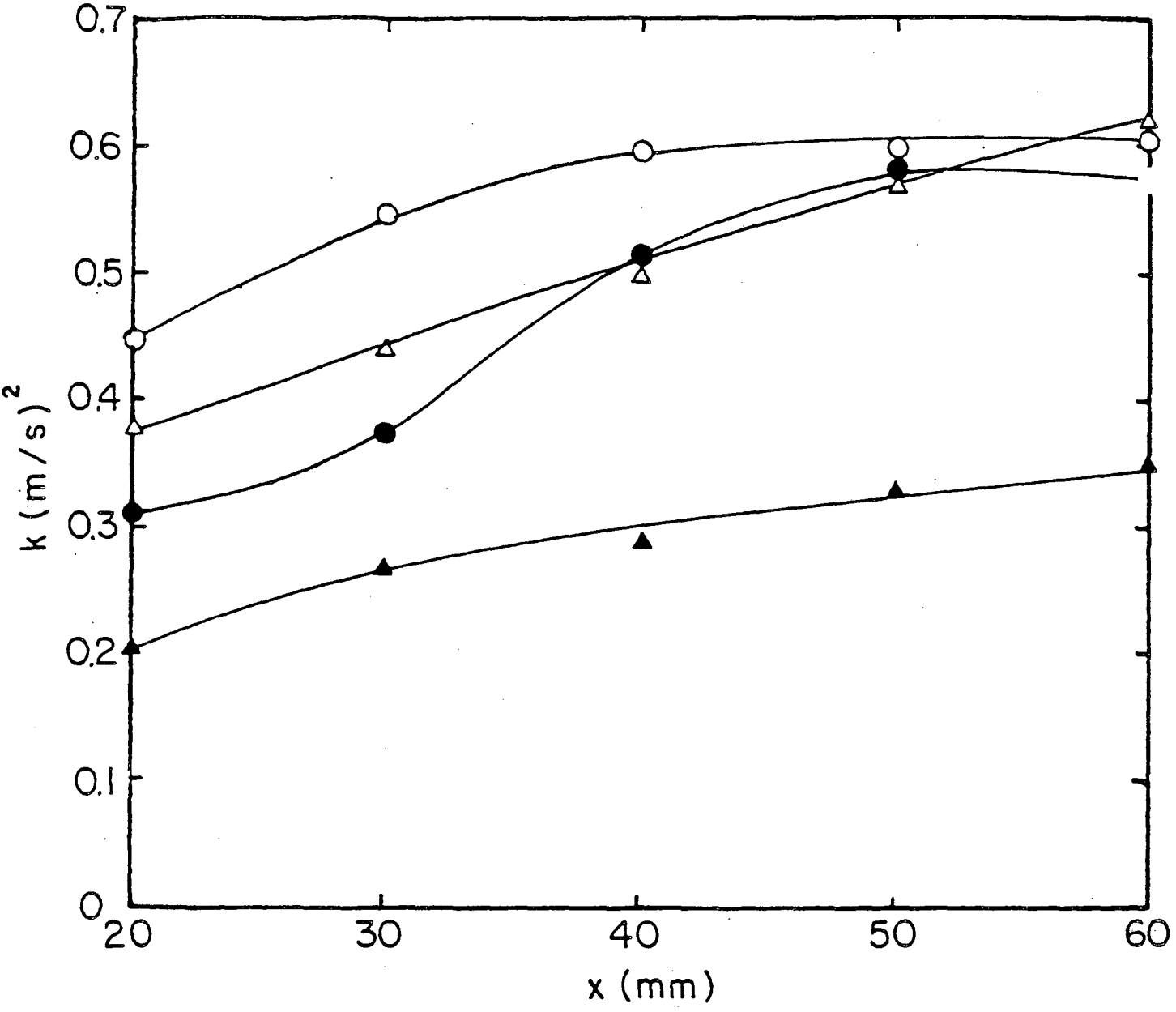

Fig. 7 k_{max} as function of x. No. 1, ●; No. 2, ○, No. 3, ▲; No. 4, △.

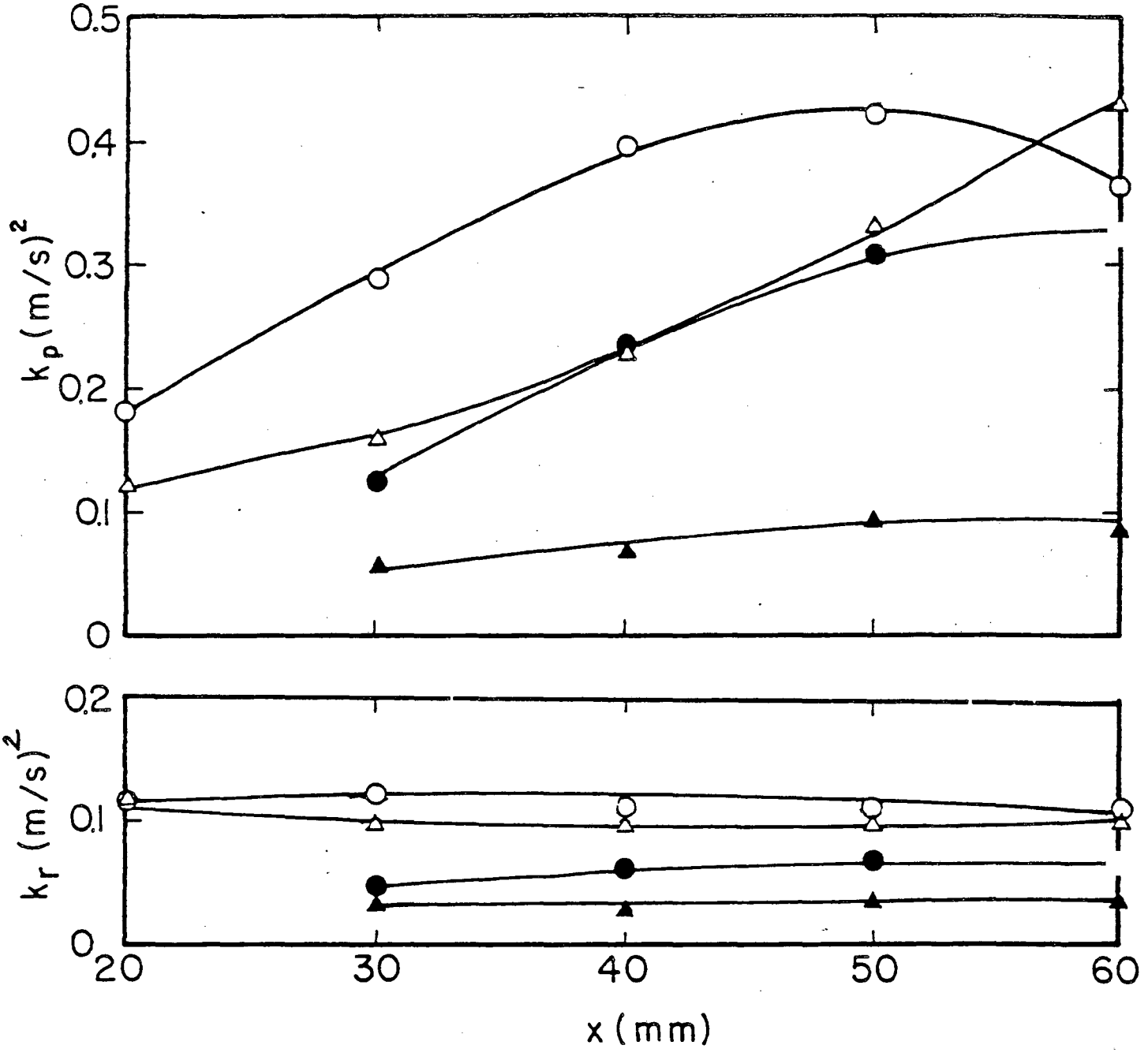

Fig. 8 Conditioned turbulent kinetic energy in the reactants, k_r, and in the products, k_p, associated with k_{max}. No. 1, ●; No. 2, ○, No. 3, ▲; No. 4, △.

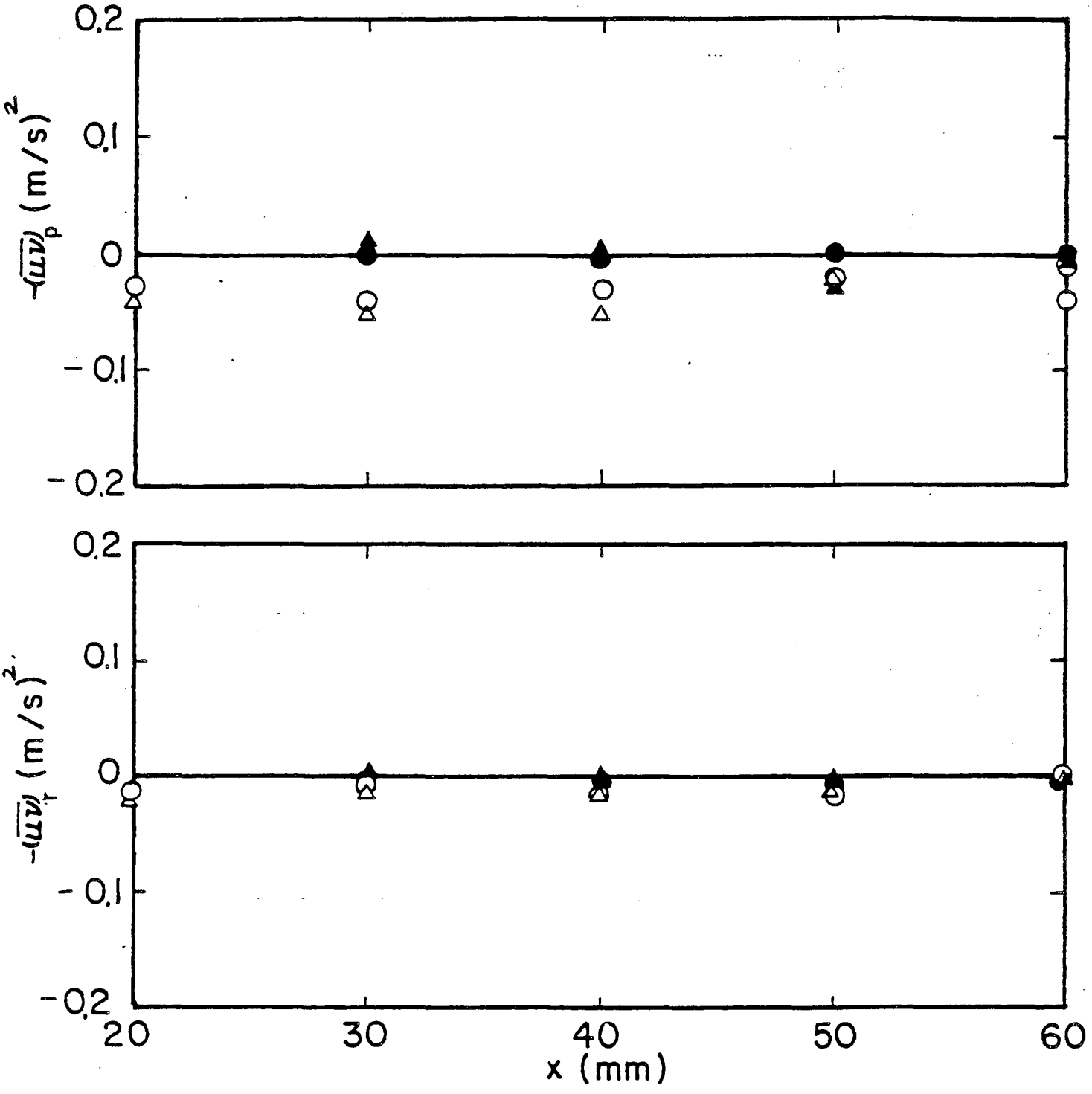

Fig. 9 Conditioned Reynolds stress in the reactants $-\overline{(uv)}_r$, and in the products, $-\overline{(uv)}_p$, associated with k_{max}. No. 1, ●; No. 2, ○, No. 3, ▲; No. 4, Δ.

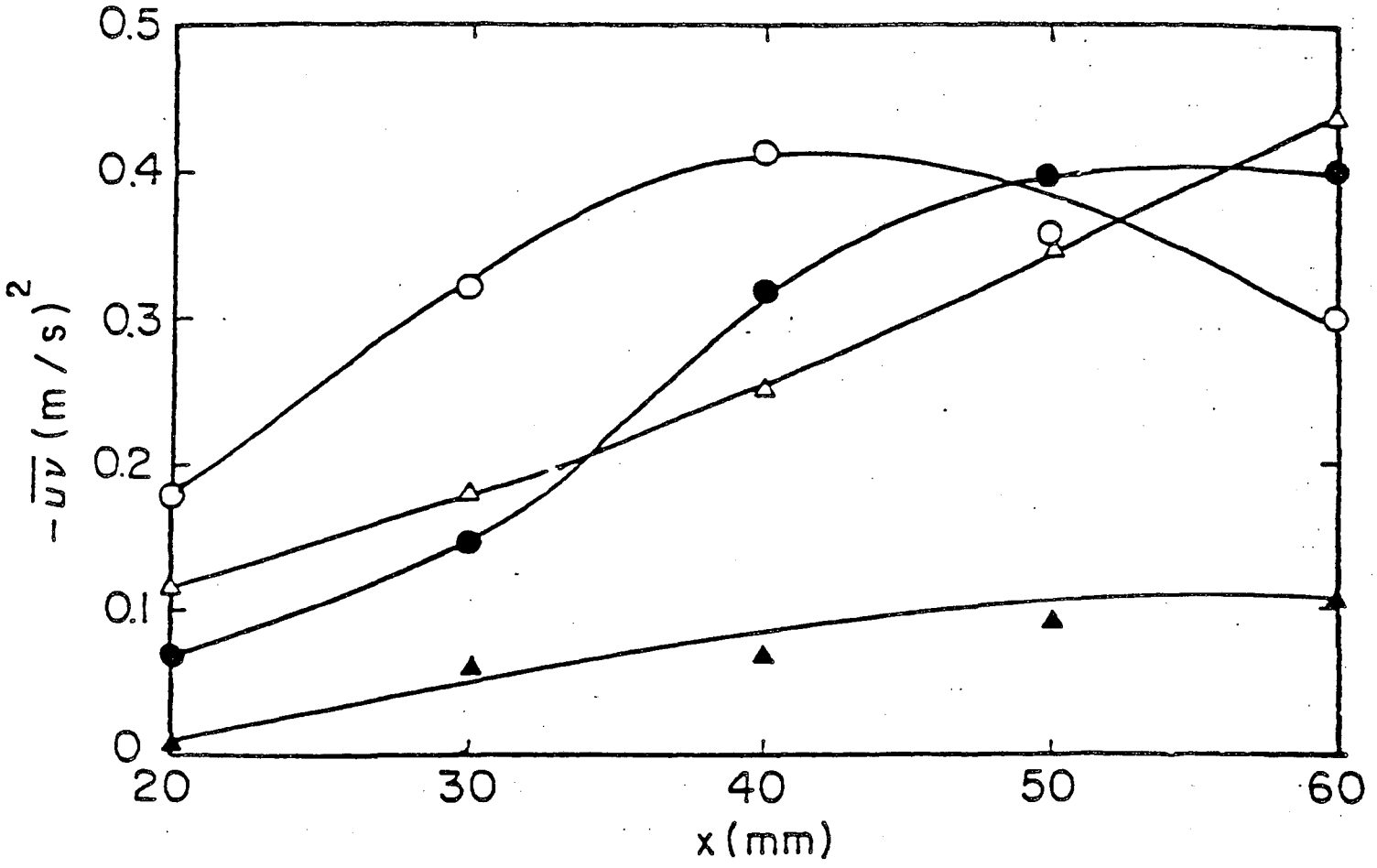

Fig. 10 Unconditioned Reynolds stress $-\overline{uv}$ associated with k_{max}. No. 1, ●; No. 2, ci , No. 3, ▲; No. 4, Δ.

TECHNICAL INFORMATION DEPARTMENT
LAWRENCE BERKELEY LABORATORY
UNIVERSITY OF CALIFORNIA
BERKELEY, CALIFORNIA 94720